Volume 9, Issue 6, 2019, 4452 - 4457 ISSN 2069-5837

Biointerface Research in Applied Chemistry

www.BiointerfaceResearch.com

https://doi.org/10.33263/BRIAC96.452457

Original Research Article Open Access Journal

Received: 22.08.2019 / Revised: 14.10.2019 / Accepted: 18.10.2019 / Published on-line: 21.10.2019

Determining the molecular-weight and interfacial properties of chitosan built nanohydrogel for controlled drug delivery applications

Faheem Ullah [1], Fatima Javed [2], Muhammad Razlan Zakaria [1], Nargis Jamila[2], Rozina Khattak[2], Abdul Naeem Khan [3], Hazizan Md. Akil [1,*]

[1]School of Materials and Mineral Resources Engineering, Universiti Sains Malaysia, Seri Ampangan, 14300 Nibong Tebal, Pulau Penang, Malaysia
[2]Department of Chemistry, Shaheed Benazir Bhutto Women University, Peshawar, Pakistan
National; Centre of Excellence in Physical Chemistry, University of Peshawar, 25120, Pakistan

*corresponding author e-mail address: ***hazizan@usm.my*** |Scopus ID 7102836574

ABSTRACT

Recent development in polymeric nanohydrogel demands surface modification, interfacial properties and determination of molecular weight for effective drug loading and release studies. Therefore, chitosan built nanohydrogel were synthesized via free radical copolymerization and functionalized with hydrophilic ligands to act as amphiphilic diblock copolymers in aqueous medium. The investigated properties like porosity (61- 73 %) , cross-linking density (20.38- 25.22), critical micelle concentration (CMC≈ 0.41- 0.62 g/L), thermodynamic of adsorption followed by micellization, and the molecular weight of chitosan built nanohydrogel (M_w ≈11.59-13.05 x 10^5 (g/mol, determined by applying Debye plot) have been investigated as a new tool to understand the art and chemical identity of hydrogel at air- water interface in aqueous medium regarding controlled drug delivery applications.

Keywords: *Nanohydrogel; porosity and crosslinking-density; surface tension and CMC; molecular weight and Debye plot.*

1. INTRODUCTION

Currently, chitosan built nanohydrogel serves best to fulfill the highly demanding controlled drug delivery applications, but it is necessary to modify the said hydrogel to interact with various drugs and cellular environment at physiological conditions. Surface modification of chitosan built hydrogel by using hydrophilic ligands can add to the association, diffusion and interaction of hydrogel with hydrophilic and hydrophobic drugs at air-water interface [1-3]. Further, to understand the synthetic chemistry, low-temperature treatment, the surface properties, identification of pendant groups, interfacial properties and molecular- weight has no matching if explored properly.

Currently, the basic criteria to develop hydrogel for controlled drug delivery applications is to concentrate on biomaterials with biodegradable and biocompatible properties with no side-effect on the accumulation in the body as compared to metallic nanoparticles or synthetic chemicals [4-6]. To highlight this theme, the most promising chitosan and starch were considered as the starting material to fabricate chemically- crosslinked hydrogel networks. The resultant repulsion of pendant group in chitosan will assist in association, solubilization, swelling where the relevant chains interact with oppositely charged cellular surfaces, drug and biomolecules through various electrostatic interactions. Chitosan is known to protect the drug from hostile as well as antagonistic environment, its efficient removal through renal filtration and enzymatic degradation [7-10]. Starch is introduced as a new material to produce interpenetrating hydrogel networks and known as the most common polymeric carbohydrate with graftable properties to produce functional materials. In pharmaceutical industry, starch is used as safe tablet disintegrant, binder and a long-term stabilizing agent as expedient [11-13]. So, the combination of chitosan and starch addressed as healthy biomaterials to produce safe, biocompatible and functional hydrogel for controlled drug delivery applications. As both the materials have promising properties but lack the ability to interact with hydrophobic drug in aqueous medium due to hydrophilic/ hydrophobic imbalance and poor association. Thus, to induce an amphiphilic balance, the hydrogel was functionalized by hydrophilic moieties like pthalic-anhydride (PA) and hexamethylenetetramine (HMTA) to self-associate and interact with hydrophobic drugs at air-water interface in the form of self-organized micelles [14, 15]. The selective functional moieties are also described with biocompatible properties as PA is considered as versatile intermediate in organic chemistry and used in the pharmaceutical industry with antiviral properties [16, 17]. Also HMTA is a heterocyclic organic compound, soluble in water only at acidic conditions, having a cage-like structure used as preservative and to treat urinary tract infection.

The objective of this work is synthesis and functionalization of chitosan built nanohydrogel, its determination of molecular weight (by using Debye plot) and interfacial properties (by using tensiometry) for controlled drug delivery applications.

2. MATERIALS AND METHODS

2.1. Synthesis, and surface modification of chitosan built nanohydrogel.

Chitosan built nanohydrogel were successfully synthesized via repeatedly free- radical copolymerization method followed by successive functionalization [18, 19]. As shown in **Figure 1**, the

synthetic reaction was accomplished at 78 ^{o}C by using thermal initiator system with a newly introduced cross-linker known as carbohidrizide (CZ). After some time the system became progressively thicker and was observed until it could not be stirred. The resultant hydrogel was purified by centrifugation, decantation and frequently washing with DDH_2O [20]. Finally the hydrogel was purified at room temperature by dialysis for 07 days in membrane tubing (Spectrum laboratories, Inc., Rancho Dominguez, CA, USA; MW cutoff 12,000–14,000). The product was de-watered using ethanol for 2 h, cut into small pieces, gronded and over washed with ethanol followed by storing in absence of heat, light and moisture. The native hydrogel was then functionalized with pthalic-anhdride (PA) and hexaethylenteteramine (PA) via 1-Ethyl-3-(3-dimethylaminopropyl) carbodimide (EDC) catalyzed coupling of PA and HMTA to replace -OH groups in CS units followed by dialysis for 10 to remove all the unreacted moieties. The feed composition is shown in **Table 1.**

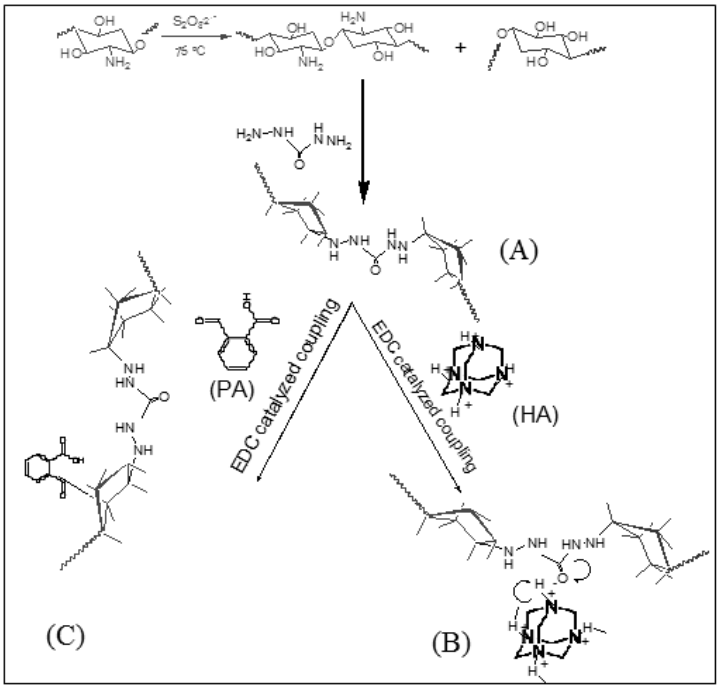

Figure 1. Synthesis and surface modification of chitosan built nanohydrogel with induced hydrophilic ligands to work as amphiphilic block copolymers in aqueous medium.

2.2. Structure confirmation by solid state C^{13}- NMR analysis.

In comparison to liquid- state ^{13}C-NMR studies, the peaks in solid-state NMR spectra are very broad due to bulky group, anisotropic and orientation effects. Further, the intensity of peak lines is greatly affected due to low sensitivity and poor resolution as several peaks overlap each other in the solid state. The experimentally-determined solid state ^{13}C NMR spectra of functionalized hydrogel samples coded as B and C are revealed in **Figure 2** respectively. The experimental peaks were compared with the reported literature [1, 21]. The desirable and characteristic peak for -C-NH_2 is observed at 35-45 ppm **(a),** representing amine functionality in chitosan, responsible for swelling and de-swelling for controlled- drug loading and release profiles at physiological pH (near pKa≈ 6.54 of chitosan). The resonance peak for –CH_2 40-46 ppm **(b)**, -C-OH 50-55 ppm **(c)**, -C-N 80-85 **(d),** amides 175-185 ppm **(e)**, carbonyl 190-200 ppm **(f)** could be attributed to the reaction between CS, SR and the chemical crosslinker carbohydrizide. The hydrogel functionalized with Hexamethylentetramine (B), has been verified by shifting of peaks and appearance of an additional peak for heterocyclic ring (combination of C-N,-CH_2, -N-C-N groups) in the range of 210-230 ppm. In case of hydrogel functionalized with pthaic-anhydride (C), the appearance of peak for aromatic stretching around 200 ppm and absence of heterocylic ring (in comparison to (B) is a direct clue of the carbon resonance could be credited to the degree of crosslinking and induced hydrophilicity.

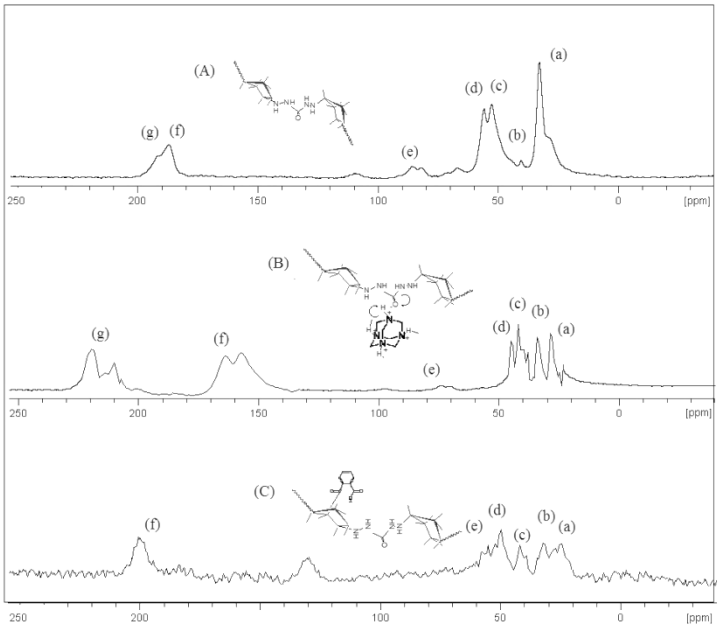

Figure 2. Solid state ^{13}C NMR confirmation of native and functionalized chitosan built nano hydrogel.

Table 1. Feed composition of hydrogel native (A), functionalized with PA(B) and HMTA(C).

Sample Code	Chitosan (mg)	Starch (mg)	CZ (M)	APS (M)	EDC (mg)	Curing hours	Curing temp ^{o}C	Curing Dialysis (days)
A	600	400	0.5	0.5	-	23.5	78	17
B	600	400	0.5	0.5	150	15	25	17
C	600	400	0.5	0.5	150	15	25	17

3. RESULTS

3.1. Significant properties of chitosan-stach based nanoydrogel. The significant properties of hydrogel including swelling, porosity, crosslinking density and quality of solvent (water) can be fully understood by applying Flory–Rehner's

equation. Further, the porosity, number of pores, equilibrium swelling, equilibrium volume friction of hydrogel and average molecular weight of a chain between adjacent crosslinking point can be numerically calculated by using several equations including Flory–Rehner equation [22] as:

$$Porosity\% = [1-\{\frac{F}{\frac{\rho}{P}}\}]X100 \quad \textbf{(Eq. 1)}$$

$$Equilibrium-Swelling = \frac{V1+V2}{V2} = \frac{\frac{\omega_1}{\rho_1}+\frac{\omega_2}{\rho_2}}{\frac{\omega_2}{\rho_2}} \quad \textbf{(Eq. 2)}$$

$$Polymer-volume-friction(\nu_P) = Q^{-1} \quad \textbf{(Eq. 3)}$$

Flory-Rehner equation was assumed based on the quilibrium swelling of polymeric hydrogel in aqueous environment. The Flory-Rehner equation is given as **Eq. 4** [23]

$$-[\ln(1-\nu_P)+\nu_P+\chi{\nu_P}^2] = NV_S[{\nu_P}^{1/3}-\frac{\nu_P}{2}] \quad \textbf{(Eq. 4)}$$

where N is the crosslinking density (mol/m^3), V_S is the molar volume of the solvent ($H_2O\approx$ 18.03 ml/mol). Using 0.5 as the interaction parameter of χ. The crosslinking density N and the average molecular weight of a chain between adjacent crosslinking points M_c were calculated by Using **Eq. 5** [24]

$$-[\ln(1-\nu_P)+\nu_P+\chi{\nu_P}^2] = \frac{\rho_2}{M_c}V_S.{\nu_P}^{1/3} \quad \textbf{(Eq. 5)}$$

It should be pointed out that ρ_2 was replaced with the experimentally measured density of each hydrogel, which was 2.25 g/cm^3 for medium molecular weight. The solvent density ($H_2O\approx$ 1.01 g/cm^3) with molar volume of 18.03 cm^3 /mol. The value χ for copolymerized chitosan was estimated as 0.5 accordingly [25]. Such numerical investigations have significant effects regarding physicochemical and drug administration aspects of chitosan built hydrogel for controlled drug delivery applications. The summary of significant physical properties is shown in **Table 2.** An increase in density reflects the effective functionalization whereas the increase in porosity is attributed to the interaction of hydrophilic ligands to overcome the electrostatic attraction between chitosan and starch molecules and development of new junctions and interactions. The respective decrease in polymer volume friction, molecular weight of the adjacent crosslinked chain and crosslinking density is attributed to the development of new interfaces and junction points with the successive functionalization which are the characteristic properties of the proposed strategy. These parameters are necessary to explore the hidden chemistry of hydrogel technology for efficient drug delivery.

3.2. Interfacial properties of chitosan built nanohydrogel.

Critical micelle concentration (CMC) is determined from the break point of the plot of surface tension versus log of the concentration of hydrogel in aqueous medium. The thermodynamic parameters of micellization can be calculated from CMC value. The relation of different thermodynamic parameters with CMC can be derived using different equations. The thermodynamics of micellization is governed by the molecular structure of neutral hydrogel particles. The reduction in free energy associated with the movement of hydrophobic parts from an aqueous to micellar environment can be determined by the variation of the CMC with respect to the hydrophobic chain. The hydrophilic groups can be utilized to determine the free energy change associated with micellization of hydrophobic block [26, 27].

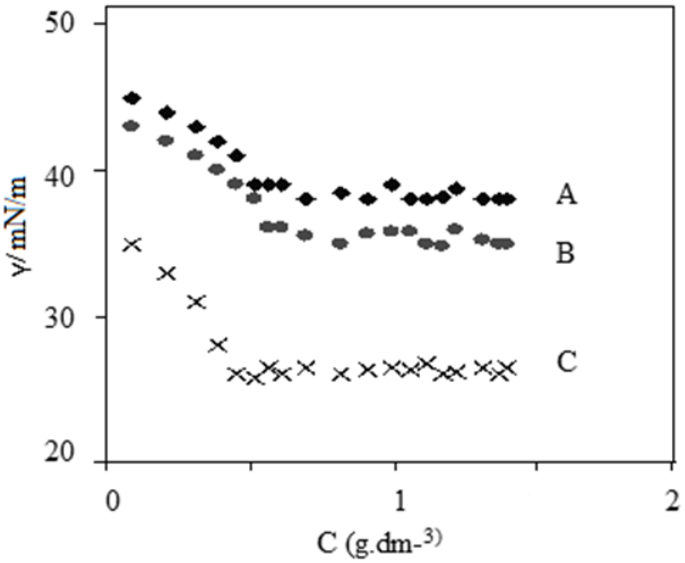

Figure 3. Plot of surface tension (γ) as a function of concentration for native (A) and functionalized (B, C) hydrogel at 37 ^{o}C.

A gradual decrease in the surface tension of hydrogel solution was attributed to the formation of complete Gibbs's monolayer indicating the onset of micellization as shown in **Figure 3**. The CMC determination deals with bulk of solution and the non constant behavior of surface tension after CMC reflects the dynamic nature of micellization [28]. The thermodynamic parameters of micellization like ΔG_{mic}, ΔH_{mic} and ΔS_{mic} for native and functionalized nanohydrogel solutions are shown in **Table 3.** The negative values of ΔG_{mic} suggest micellization as a spontaneous process. ΔH_{mic} is positive in all cases, indicating the process is endothermic. Also, small values of ΔH_{mic} shows that no bond breaking and new-bond-formation take place during micellization. Thus, micellization is a physical process and only physical interaction takes place between the solute, solvent and bioactive species. During the process of micellization, the entropy change is always positive as the structure of water molecules is affected as hydrophobic blocks are removed from the aqueous bulk to the interior of micelle and also the freedom of hydrophobic block in the interior of micelle is increased. Finally, the process shows that adsorption occurs followed by the micellization respectively [29].

3.3. Determination of Molecular weight by using Debye plot.

Static light scattering is a useful technique that uses the intensity traces at a number of angles to get information about the molecular mass (M_w), radius of gyration (R_g) and second viral coefficient (A_2) of polymer and polymer-complexes. A simple static light scattering experiment entails the average intensity of the sample that is corrected for the scattering of the solvent will yield the Rayleigh ratio, R as a function of the angle or the wave vector q as following [30].

$$R(\theta_{sample}) = R(\theta_{solvent})I_{sample}/I_{solvent} \quad \textbf{(Eq. 6)}$$

The difference in the Rayleigh ratio ΔR (θ) between the sample and solvent is given by the equation

$$\Delta R(\theta) = R(\theta_{sample}) - R(\theta_{solvent}) \quad \textbf{(Eq. 7)}$$

In addition, the setup of laser light scattering is corrected with a liquid of known refractive index and Rayleigh ratio e.g. toluene, benzene or decline. The data analysis has been performed without a so-called material constant K, which can lead to the calculation of other physical parameters of the system and is defined below.

$$K = 4\pi^2 n_o^2 (dn/dc)^2 / N_A \lambda^4 \quad \textbf{(Eq. 8)}$$

Where (dn/dc) is the refractive index increment, n_o is the refractive index of the solvent, N_A is Avogadro's number and λ is the wavelength of the laser light scattering reaching the detector.

Debye plot is employed for dilute solutions of polymer (hydrogel), where additional scattering arises from concentration fluctuation, which is given by Rayleigh Gans Debye as;

$$\Delta R_\theta = KcM \quad \textbf{(Eq. 9)}$$

Where, ΔR_θ = Excess Rayleigh function

c = Concentration,

M = molar mass, K = optical constant.

For dilute solutions of low molecular weight average molar mass M_w (for particle smaller than λ/20) the above equation can be modified as [31];

$$\frac{KC}{\Delta R_\theta} = \frac{1}{M_w} + 2A_2C \quad \textbf{(Eq. 10)}$$

This method is used to derive the molecular mass (M_w), and second viral coefficient(A_2) of polymer or polymer complex system by plotting a graph between KC/R_θ vs C.

As per measurement, value of the apparent hydrodynamic radius of micelle decreases with increase of concentration for all hydrogel solutions. It is due to repulsive interaction between the outer portions of micelles in bulk. When number of micelles in the system is increased, then they come close to each other and as a result of this closeness, their sizes are reduced. So reduction in the size is due to the increase in number of micelles in the system. The number of micelle increases with addition of hydrogel in solution. Micelles already present in bulk, reduce their size to accommodate new micelles in the system [32, 33]

Measurement of scattered light was performed at θ= 90° in the temperatures ranges from 20-50 ºC at various concentrations. The data from static light scattering was analyzed by using Debye's equation. Debye plots were used to obtained apparent molar mass M_w and second virial coefficient A_2 from the intercept and slope of the plots respectively as shown in **Figure 4**. At very low concentration, the polymer molecules are predominantly in the un-associated state. On increasing the concentration of hydrogel, the scattering intensity increases rapidly over a narrow concentration range, reflecting additional light scattering, which arises from solute concentration in solution. This indicates that formation of micelles is strongly favored [34].

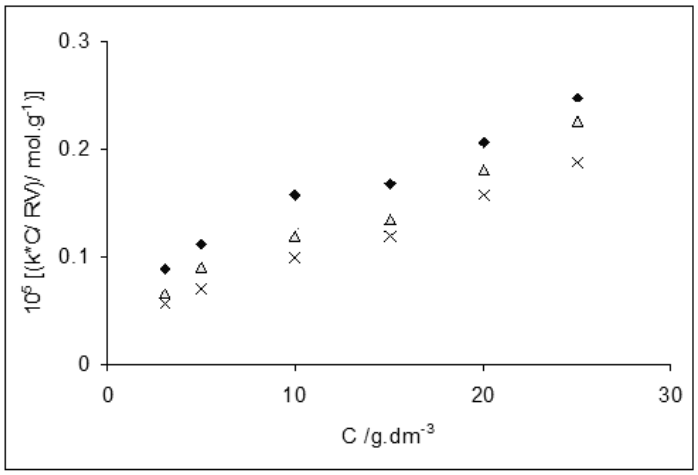

Figure 4. Debye plot for native and functionalized hydrogel in aqueous solutions at 37 °C.

For hydrogel solutions, the increase in apparent molar mass and association number with an increase in temperature is attributed to the fact that at high temperature the solvent becomes poorer for the hydrogel and micellization is preferential. The association number was effected inversly by hydrophilic functional moieties as the greater the hydrophobicity more is the association and self-organization to form micelles. The higher association number means that micelle is much harder this is due to the fact that at high temperature the solvent becomes poorer for hydrogel and micellization is preferential [35, 36]. Another parameter obtained from Debye plot is the second virial coefficient (A_2) and its values are given in **Table 4.** It is clear that for all hydrogel solutions, the values of A_2 decreases with the increase in temperature because, at high temperature, the solvent becomes poorer and solvent-solute interaction decreases. The hydrophilic ligands directly affect the values of A_2, as the polymer-solvent increased with the functionalization. At higher temperature the hydrogel units were observed in dehydrated form and preferred to gather in hydrophobic environment of the micelle instead of remaining in the hydrophilic bulk in order to maintain the hydrophilic-hydrophobic balance [37, 38].

Table 2. Significant parameters of native and functionalized nanohydrogel.

Hydrogel Code	Density (g/cm^3)	Porosity (%)	Polymer volume friction ($v_{P)}$	$M_w$of adjacent crosslink chain (M_c/ $kg.mol^{-1}$)	Crosslinking density ($mol.\ m^3$)
A	2.25	61	0.036	3.22	25.22
B	2.55	70	0.031	3.11	22.19
C	2.61	73	0.028	2.99	20.38

Table 3. Interfacial and thermodynamic properties of native and functionalized hydrogel.

Hydrogel code	CMC (g/L)	ΔG_{mic} (Kj/mol)	ΔH_{mic} (Kj/mol)	ΔS_{mic} (Kj/mol)	ΔS_{mic} (Kj/mol)	$\Gamma/10^{-10}$ (mol/cm^2)	ΔG_{ads} (Kj/mol)	ΔH_{ads} (Kj/mol)	ΔS_{ads} (Kj/mol)
A	0.62	-22.50	13.53	0.124	0.124	2.14	-28.27	121.14	0.611
B	0.54	-18.53	12.88	0.124	0.124	2.13	-25.14	121.32	0.611
C	0.41	-16.55	12.56	0.124	0.124	2.15	-22.44	121.08	0.611

Table 4. Determination of moleculear weight second virial coefficient and hydrodynamic radius by using Laser Light Scattering at 37 ^{o}C.

Hydrogel code	T /(K)	*dn/dc* (L/ g)	T /(K)	M_w x 10^5 (g/mol)	A_2 x 10^{-4} (mol.ml.g^{-2})	R_h (nm)
A	310	2.53	310	13.05	2.45	22.58
B	310	2.41	310	12.07	11.25	14.85
C	310	2.25	310	11.59	15.87	9.54

4. CONCLUSIONS

Chitosan-co-starch based nanohydrogel were successfully synthesized followed by surface modification with pthalic-anhydride and hexamethylenetetramine via EDC catalyzed carbodimide coupling respectively. With the successive functionalization, the significant properties like density and porosity increases, and a corresponding decrease in crosslinking density was observed due to the formation of hydrophilic contacts with aqueous environment at physiological conditions. The determination of molecular weight (M_w ≈11.59- 13.05 x 10^5 (g/mol) and interfacial properties like CMC ≈ 0.41-0.62 g/L**)is** considered as a new tool to tune the hydrogel as promising and desirable hydrophobic drug carriers.

5. REFERENCES

1. Ullah, F.; Javed, F.; Othman, M.B.H.; Khan, A.; Gul, R.; Ahmad, Z.; Md Akil, H. Synthesis and functionalization of chitosan built hydrogel with induced hydrophilicity for extended release of sparingly soluble drugs. *Journal of Biomaterials Science, Polymer Edition* **2018**, *29*, 376-396, https://doi.org/10.1080/09205063.2017.1421347.
2. Sami El-banna, F.; Mahfouz, M. E.; Leporatti, S.; El-Kemary, M.; AN Hanafy, N. Chitosan as a natural copolymer with unique properties for the development of Hydrogels. *Applied Sciences* **2019**, *9*(11), 2193, https://doi.org/10.3390/app9112193.
4. 3. Amini-Fazl, M.S.; Mohammadi, R.; Kheiri, K. 5-Fluorouracil loaded chitosan/polyacrylic acid/Fe3O4 magnetic nanocomposite hydrogel as a potential anticancer drug delivery system. *International Journal of Biological Macromolecules* **2019**, *132*, 506-513, https://doi.org/10.1016/j.ijbiomac.2019.04.005.Ahmed, T.A.; Aljaeid, B.M. Preparation, characterization, and potential application of chitosan, chitosan derivatives, and chitosan metal nanoparticles in pharmaceutical drug delivery. *Drug Design, Development and Therapy* **2016**, *10*, 483, https://doi.org/10.2147/DDDT.S99651.
5. Chen, J.C.; Li, L.M.; Gao, J.Q. Biomaterials for local drug delivery in central nervous system. *International Journal of Pharmaceutics* **2019**, *560*, 92-100, https://doi.org/10.1016/j.ijpharm.2019.01.071.
6. Ahmad, S.; Ahmad, M.; Manzoor, K.; Purwar, R.; & Ikram, S. A review on latest innovations in natural gums based hydrogels: Preparations & applications. *International Journal of Biological Macromolecules* **2019**, 136, 870-890, https://doi.org/10.1016/j.ijbiomac.2019.06.113.
7. Gorgieva, S.; Kokol, V. Preparation, characterization, and in vitro enzymatic degradation of chitosan-gelatine hydrogel scaffolds as potential biomaterials. *Journal of Biomedical Materials Research Part A* **2012**, *100*, 1655-1667, https://doi.org/10.1002/jbm.a.34106.
8. Delmar, K.; Bianco-Peled, H. Composite chitosan hydrogels for extended release of hydrophobic drugs. *Carbohydrate Polymers* **2016**, *136*, 570-580, https://doi.org/10.1016/j.carbpol.2015.09.072.
9. Ullah, F.; Javed, F.; Othman, M.B.H.; Ahmad, Z.; Akil, H.M. Synthesis and physicochemical investigation of chitosan-built hydrogel with induced glucose sensitivity. *International Journal of Polymeric Materials and Polymeric Biomaterials* **2017**, *66*, 824-834, http://dx.doi.org/10.1080/00914037.2016.1276061.
10. Liu, L.; Gao, Q.; Lu, X.; Zhou, H. In situ forming hydrogels based on chitosan for drug delivery and tissue regeneration. *Asian Journal of Pharmaceutical Sciences* **2016**, *11*(6), 673-683, https://doi.org/10.1016/j.ajps.2016.07.001.
11. Song, R.; Maxwell, M.; Chenshuang, L.; Kang, T.; Chia, S.; Zhong, Z. Current development of biodegradable polymeric materials for biomedical applications.. *Drug Design, Development and Therapy* **2018**, 12, 3117-3145, doi:10.2147/DDDT.S16544.
12. Stumpel, J.E.; Gil, E.R.; Spoelstra, A.B.; Bastiaansen, C.W.M.; Broer, D.J.; Schenning, A.P.H.J. Stimuli-responsive materials based on interpenetrating polymer liquid crystal hydrogels. *Advanced Functional Materials* 2015, 25, 3314-3320, https://doi.org/10.1002/adfm.201500745.
13. Perez, J.J.; Francois, N.J.; Maroniche, G.A.; Borrajo, M.P.; Pereyra, M.A.; Creus, C.M. A novel, green, low-cost chitosan-starch hydrogel as potential delivery system for plant growth-promoting bacteria. *Carbohydrate Polymers* **2018**, *202*, 409-417, https://doi.org/10.1016/j.carbpol.2018.07.084.
14. Larrañeta, E.; Stewart, S.; Ervine, M.; Al-Kasasbeh, R.; Donnelly, R.F. Hydrogels for hydrophobic drug delivery. Classification, synthesis and applications. *Journal of Functional Biomaterials* **2018**, *9*(1), 13, https://doi.org/10.3390/jfb9010013.
15. Darge, H.F.; Andrgie, A.T.; Tsai, H.C.; Lai, J.Y. Polysaccharide and polypeptide based injectable thermo-sensitive hydrogels for local biomedical applications. *International Journal of Biological Macromolecules* 2019, 133, 545-563, https://doi.org/10.1016/j.ijbiomac.2019.04.131.
16. Plotnikov, V.M. Anti-tumoral, antibacterial and antiviral pharmaceutical composition (variants). *Google Patents* **2009**.
17. Ullah, F.; Othman, M.B.H.; Javed, F.; Ahmad, Z.; Akil, H.M. Classification, processing and application of hydrogels: A review. *Materials Science and Engineering: C* **2015**, *57*, 414-433, https://doi.org/10.1016/j.msec.2015.07.053.
18. Dash, M.; Chiellini, F.; Ottenbrite, R.M.; Chiellini, E. Chitosan—A versatile semi-synthetic polymer in biomedical applications. *Progress in Polymer Science* **2011**, *36*, 981-1014, https://doi.org/10.1016/j.progpolymsci.2011.02.001.
19. Ullah, F.; Othman, M.B.H.; Javed, F.; Ahmad, Z.; Akil, H.M.; Rasib, S.Z.M. Functional properties of chitosan built nanohydrogel with enhanced glucose-sensitivity. *International*

Journal of Biological Macromolecules **2016**, *83*, 376-384, https://doi.org/10.1016/j.ijbiomac.2015.11.040.

20. Rasib, S.Z.M.; Akil, H.M.; Khan, A.; Hamid, Z.A.A. Controlled release studies through chitosan-based hydrogel synthesized at different polymerization stages. *International Journal of Biological Macromolecules* **2019**, *128*, 531-536, https://doi.org/10.1016/j.ijbiomac.2019.01.190.

21. Kono, H.; Teshirogi, T. Cyclodextrin-grafted chitosan hydrogels for controlled drug delivery. *International Journal of Biological Macromolecules* **2015**, *72*, 299-308, https://doi.org/10.1016/j.ijbiomac.2014.08.030.

22. Elliott, J.E.; Macdonald, M.; Nie, J.; Bowman, C.N. Structure and swelling of poly (acrylic acid) hydrogels: effect of pH, ionic strength, and dilution on the crosslinked polymer structure. *Polymer* **2004**, *45*, 1503-1510, https://doi.org/10.1016/j.polymer.2003.12.040.

23. Flory, P.J. *Principles of polymer chemistry*. Cornell University Press, 1953.

24. Xia, Z.; Patchan, M.; Maranchi, J.; Elisseeff, J.; Trexler, M. Determination of crosslinking density of hydrogels prepared from microcrystalline cellulose. *Journal of Applied Polymer Science* **2013**, *127*, 4537-4541, https://doi.org/10.1002/app.38052.

25. Baier, L.J.; Bivens, K.A.; Patrick, C.W.Jr.; Sxhmidt, C.E. Photocrosslinked hyaluronic acid hydrogels: natural, biodegradable tissue engineering scaffolds. *Biotechnology and Bioengineering* **2003**, *82*, 578-589, https://doi.org/10.1002/bit.10605.

26. Zdziennicka, A.; Szymczyk, K.; Krawczyk, J.; Janczuk, B. Critical micelle concentration of some surfactants and thermodynamic parameters of their micellization. *Fluid Phase Equilibria* **2012**, *322*, 126-134, https://doi.org/10.1016/j.fluid.2012.03.018.

27. Ullah, F.; Khan, A.; Akil, H.M.; Siddiq, M. Effect of hydrophilic/hydrophobic block ratio and temperature on the surface and associative properties of oxyethylene and oxybutylene diblock copolymers in aqueous media. *Journal of Dispersion Science and Technology* **2015**, *36*, 1777-1785, https://doi.org/10.1080/01932691.2015.1019625.

28. Khan, A.; Bibi, I.; Pervaiz, S.; Mahmood, K.; Siddiq, M. Surface tension, density and viscosity studies on the associative behaviour of oxyethylene-oxybutylene diblock copolymers in water at different temperatures. *International Journal of Organic Chemistry* **2012**, *2*, 82-92, https://doi.org/10.4236/ijoc.2012.21014.

29. Toomey, R.; Mays, J.; Yang, J.; Tirrell, M. Postadsorption rearrangements of block copolymer micelles at the solid/liquid interface. *Macromolecules* **2006**, *39*, 2262-2267, https://doi.org/10.1021/ma051097i.

30. Brar, S.K.; Verma, M. Measurement of nanoparticles by light-scattering techniques. *TrAC Trends in Analytical Chemistry* **2011**, *30*, 4-17, https://doi.org/10.1016/j.trac.2010.08.008.

31. Young, R.J.; Lovell, P.A. Introduction to polymers. *CRC press* **2011**.

32. Bae, Y.; Jang, W.D.; Nishiyama, N.; Fukushima, S.; Kataoka, K. Multifunctional polymeric micelles with folate-mediated cancer cell targeting and pH-triggered drug releasing properties for active intracellular drug delivery. *Molecular BioSystems* **2005**, *1*, 242-250, https://doi.org/10.1039/b500266d.

33. Luo, M.; Jia, Z.; Sun, H.; Liao, L.; Wen, Q. Rheological behavior and microstructure of an anionic surfactant micelle solution with pyroelectric nanoparticle. *Colloids and Surfaces A: Physicochemical and Engineering Aspects* **2012**, *395*, 267-275, https://doi.org/10.1016/j.colsurfa.2011.12.052.

34. Almgren, M.; Brown, W.; Hvidt, S. Self-aggregation and phase behavior of poly (ethylene oxide)-poly (propylene oxide)-poly (ethylene oxide) block copolymers in aqueous solution. *Colloid and Polymer Science* **1995**, *273*, 2-15, https://doi.org/10.1007/BF00655668.

35. Chaibundit, C.; Ricardo, N.M.P.S.; de Costa, F.M.L.L.; Yeates, S.G.; Booth, C. Micellization and gelation of mixed copolymers P123 and F127 in aqueous solution. *Langmuir* **2007**, *23*, 9229-9236, https://doi.org/10.1021/la701157j.

36. Melzak, K.A.; Mateescu, A.; Toca-Herrera, J.L.; Jonas, U. Simultaneous measurement of mechanical and surface properties in thermoresponsive, anchored hydrogel films. *Langmuir* **2012**, *28*, 12871-12878, https://doi.org/10.1021/la3019666.

37. Meng, F.; Zhong, Z.; Feijen, J. Stimuli-responsive polymersomes for programmed drug delivery. *Biomacromolecules* **2009**, *10*, 197-209, https://doi.org/10.1021/bm801127d.

38. Ullah, F.; Javed, F.; Othman, M.B.H.; Rehman, S.U.; Ahmad, Z.; Akil, H.M. Star-shaped self-assembled micelles of block copolymer [chitosan-co-poly (ethylene glycol) methyl ether methacrylate] hydrogel for hydrophobic drug delivery. *Polymer Bulletin* **2018**, 75, 2243-2264, https://doi.org/10.1007/s00289-017-2152-6.

6. ACKNOWLEDGEMENTS

This research is supported by the School of Material and Mineral Source Engineering, Universiti Sains Malaysia under the project Grant FRGS-203/PBAHAN-6071337.